# A NEW HYBRID BRUSHLESS DC MOTOR/GENERATOR WITHOUT PERMANENT MAGNET

***E. Afjei*, O. Hashemipour, M. A. Saati and M. M. Nezamabadi***

*Department of Electrical and Computer Engineering, Shahid Beheshti University*
*Tehran, Iran*
*afjei@yahoo.com – omidhash@yahoo.com – alisaati@yahoo.com*

*Corresponding Author

(**Received: July 31, 2006 – Accepted in Revised Form: March 18, 2007)**

**Abstract** The Brushless DC (BLDC) motor is a simple robust machine which has found application over a wide power and speed of ranges in different shapes and geometry. This paper briefly reviews the fundamentals behind the motor and also the different types of BLDC motors with different geometries and then presents a new configuration for BLDC motor/generator, which does not use a permanent magnet in the rotor. The proposed novel motor/generator consists of two magnetically dependent stator and rotor sets (layers), where each stator set includes nine salient poles with windings wrapped around them while, the rotor comprises of six salient poles. The magnetic field passes through a guide to the rotor then the stator and finally completes its path via the motor housing. This is a three phase motor/generator and every stator and rotor pole arcs are about $30^{\circ}$. A new power electronic converter is also presented. This topology provides bidirectional control of the current for each motor phase independently. This control scheme permits the motor to operate with any number of phases at any time. In this converter, four power switches in the form of a bridge connection for each motor phase has been utilized therefore, the motor can operate by switching different sequences for the current direction in each motor phase windings and also offers the choice of having any number of phases to be on at any time. A proto-type motor/generator and the drive circuit have been built and tested in the laboratory and the numerical and experimental results are presented. Due to the ruggedness of the proposed motor/generator in comparison with the conventional and brushless dc motors used for automobile applications, this unit looks very promising for use as an integrated motor generator for hybrid vehicle.

**Keywords** Brushless DC Motor/Generator, DC Motor/Generator, DC Motor Drive, Hybrid Brushless DC Motor

\

**چکیده** موتورهای دی سی بدون جاروبک یکی از پیشرفته ترین موتور های موجود در جهان می‌باشد. این نوع موتور ها در اشکال گوناگون، توان های مختلف و در سرعت های مختلف کاربردهای وسیعی در صنعت دارند. این مقاله به بررسی چگونگی کار کرد و همچنین بررسی انواع توپولوژی های مختلف این نوع موتور می پردازد. در این راستا یک موتور دی سی بدون جاروبک بدون استفاده از مغناطیس دایم را معرفی می‌نماید. این موتور دارای دو لایه کاملا مجزا از هم دارد. هر لایه شامل استاتور با نه قطب برجسته و روتور با شش قطب برجسته می باشد. در میان این دو لایه یک سیم بندی وجود دارد که میدان تحریک را بوجود می آورد. میدان مغناطیسه از طریق شفت موتور به روتور و از آنجا به استاتور و بالاخره مسیر خود را با عبور از پوسته موتور کامل می نماید. یک راه انداز که دارای قابلیت کنترل مستقل برای هر فاز می باشد برای این موتور معرفی می‌گردد. این موتور بصورت نرم افزاری بررسی و در آزمایشگاه ساخته و تست گردید.

## 1. INTRODUCTION

Electric motors are one the most essential components and the driving force of industry today. It is estimated that more than five billion motors are built worldwide every year. In general, there are two types of motors namely ac and dc. The ac motors are usually less expensive, rugged and have low maintenance but hard to control, on the other hand the dc motors are more expensive, but highly controllable. The conventional dc motors are highly efficient and their characteristics make them suitable for use in different applications. However, one of their drawbacks is the need for a commutator and brushes, which are subject to ware and require maintenance. When the task of commutator and brushes are replaced by solid-state switches, maintenance-free motors were realized and the new motor called brushless dc motors emerged [1]. Brushless dc motors (BLDC) are one of the motor types rapidly gaining popularity. BLDC motors are used in different industries such as, automotive, aerospace, home appliances and many industrial equipment and instrumentation for various applications[2]. The small sized motors with external rotors are widely used in visual equipment such as VCRs and audio equipment such as tape recorders and digital audio tapes (DAT), computer disc drives (HDD and DVD) and OA equipment such as copiers [3,4].

The construction of modern BLCD motors is very similar to the ac motor, known as the permanent magnet synchronous motor. BLDC motors come in single-phase [5], 2-phase and three-phase configurations [6]. Out of these, the 3-phase motors are the most popular and widely used. Figure 1 shows different configurations of motors with more than one fundamental set of coils and multiple poles.

The stator of a BLDC motor consists of stacked steel laminations with windings placed in the slots that are axially cut along the inner periphery or around stator salient poles. The rotor is made of permanent magnets and can vary from two to eight pole pairs with alternate north (N) and south (S) poles. Based on the required magnetic field density in the rotor, the proper magnetic material is chosen to make the rotor. Ferrite magnets are traditionally used to make permanent magnets. As technology advances, rare earth alloy magnets are gaining popularity. In order to make a BLDC motor rotate, the stator windings should be energized in a sequence. It is essential to know the rotor position in order to understanding as to which winding must be energized.

Due to the increasing demand for higher power and less fuel consumption in cars, the concept of starter-generators integrated into the flywheel has been considered over the past several years. It is intended to provide the starter for the thermal engine and the generator for charging car batteries and supplying the onboard equipment. Significant enhancement of vehicle driving performance and improvements in fuel economy and exhaust emissions has been demonstrated by the introduction of more-electric drive concepts for road transportation. Although the application of electrical machines and drive systems in all-electric and hybrid-electric vehicles has been widely reported in recent years [7-9], there has been a relatively slow progress in these fields due to the cost of major vehicle technological changes. However, mild hybrid solutions have been recognized as the next solution, since they are viable within the existing automotive infrastructure. The Switched Reluctance Generator (SRG) is an attractive solution for worldwide increase in the demand for electrical energy. It is low cost, fault tolerant with a rugged structure and operates with high efficiency over a wide speed range. In [10], the principle operation of SRG has been presented and the necessity for closed loop control is proven. In [11], the excitation control of SRG for maximum efficiency at single pulse mode of operation has been presented. It is important to mention that, due to the obvious differences in the stator pole configurations and arcs, the newly designed motor is not a switched reluctance motor of any kind. Therefore, the primary design procedures for the switched reluctance motor are not applicable in this case.

BLDC systems are attractive for use in many high performance industrial applications with PWM used as an efficient means of power transfer, where high torque and precision control are required. Smooth torque production requires forcing a constant current through each winding phase when its back-emf is at its peak value and turning off the current when the back-emf is changing. For bipolar excitation, a positive current is injected when the back-emf is positive and the negative current when the back-emf is negative, with each conduction period lasting $120^{\circ}$. This results in two phases of conducting current and producing torque at any instant of time. Typically, hysteresis or pulse width-modulated (PWM) current controllers are used to maintain the actual currents flowing into the motor as close as possible to the rectangular reference values. They are conventionally excited with a bipolar current which requires a six-switch inverter. The unipolar motor needs fewer electronic parts and uses a simpler circuit than the bipolar motor. For these reasons, unipolar-driven motors are widely used in low-cost instruments [12]. The simplest unipolar drive consists of a single switch in a series with each winding and a zener diode or dump resistor in the freewheeling path [13]. This drive is inefficient because the stored energy in the phases is dissipated. Better performance can be obtained by using topologies that have previously been used for driving switched reluctance motors (SRM). The C-dump Topology [14], offers full regenerative control. However, it has the disadvantage of requiring a complicated control for the dump capacitor voltage, the failure of which could be catastrophic. A buck converter-based drive for the unipolar BLDC motor was proposed in [15]. Both these topologies require a higher voltage on the dump capacitors than what is applied to the motor phases during turn-on.

Due to the bidirectional nature of current flow in the motor phase windings, the driver circuit is different from that of the switched reluctance motor drive.

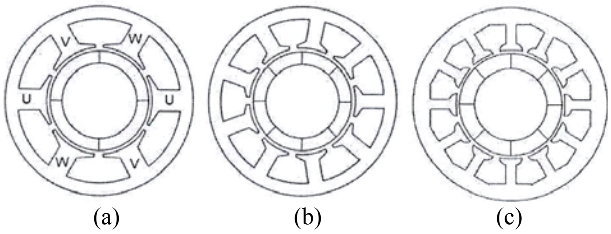


**Figure 1**. Different types of BLDC motors, (a) Four poles with two sets of coils (b) Eight poles with three sets of coils (c) Eight poles with four sets of coils.

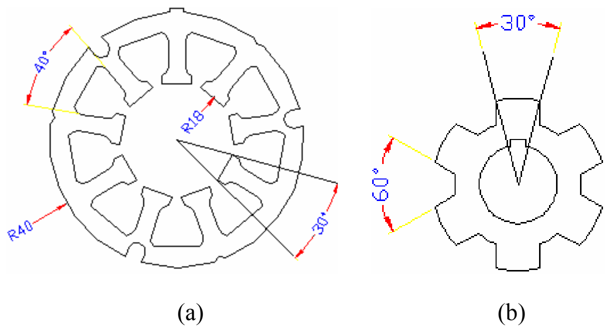


**Figure 2**. (a) Stator lamination and (b) Rotor lamination.

## 2. MOTOR/GENERATOR DESCRIPTION

The proposed novel motor consists of two magnetically dependent stator and rotor sets (layers), in which each stator set includes nine salient poles with windings wrapped around them and the rotor which comprises of six salient poles. Every stator and rotor pole arcs are $30^{\circ}$. It is worth mentioning that, the number of stator poles and their configuration is completely different than that of the switched reluctance motor. The two layers are exactly symmetrical with respect to a plane perpendicular to the middle of the motor shaft. This is a three phase motor, therefore, three coil windings from one layer is connected in series with the other three coil windings in the other layer. Figure 2 shows the shape of the stator and the rotor laminations.

There is a stationary reel, which has the field coils wrapped around it and is placed between the two-stator sets. This reel has a rotating cylindrical core, which guides the magnetic field. The magnetic flux produced by the coils travels through the guide and shaft to the rotor and then to the stator poles and finally closes itself through the motor housing. Therefore, one set of rotor poles is magnetically north and the other set is magnetically south. In this motor, the magnetic field has been induced to the rotor without using any brushes. A cut view of the motor is shown in Figure 3.

In order to get a better view of the motor configuration, the complete motor assembly is shown in Figure 4.

There are two stator and rotor sections placed on both sides of the field coil assembly which has the rotor shaft as its main core and two front/end caps plus the motor housing. A set of photo interrupters are also placed in the back of the motor for rotor position detection. One of the most widely used methods for analysis of any types of motors is the finite element technique [16].

## 3. NUMERICAL ANALYSIS

One side of the motor cross section is shown in Figure 5.

As seen from Figure 5, this motor has eight stator poles as well as six rotor poles, which will

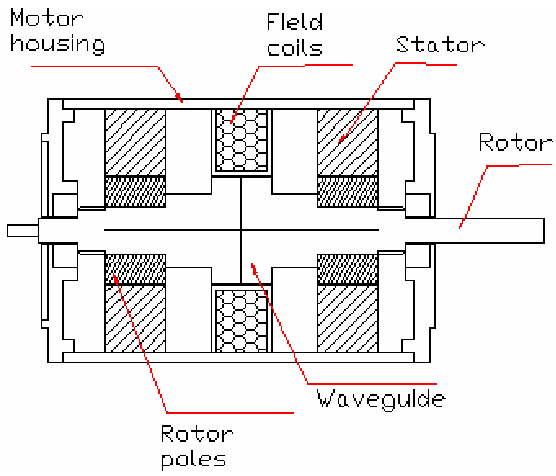


**Figure 3**. The cut view of the motor.

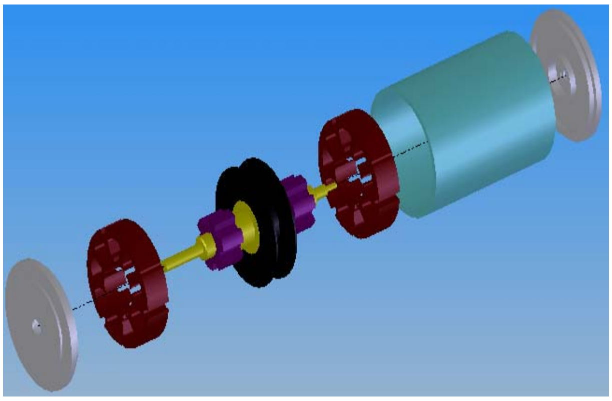

**Figure 4**. The complete motor assembly.

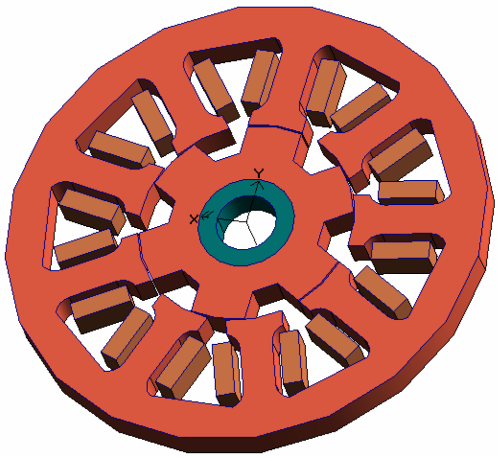

**Figure 5**. One side of the motor cross section.

be engaged in the torque production mechanism. The design of the motor becomes complicated due to complex geometry and material saturation. The reluctance variation of the motor has an important role on the performance; hence an accurate knowledge of the flux distribution inside the motor for different excitation currents and rotor positions is essential for the prediction of motor performance. The motor can be highly saturated under normal operating conditions. To evaluate properly the motor design and performance a reliable model is required. The finite-element technique can be conveniently used to obtain the magnetic vector potential values throughout the motor in the presence of complex magnetic circuit geometry and nonlinear properties of the magnetic materials. These vector potential values can be processed to obtain the field distribution, torque and flux leakage.

In order to be able to analyze this motor in a 2-D case, only one side of the motor which is symmetric to the field coil, is considered. Normal boundary conditions are applied to the outer and inner borders of the motor and a magnet producing the same magnetic field density is considered to act as the field coil. It is worth mentioning that the other options for the field coils could have been using small coil windings on the rotor poles.

The field analysis took place using a Magnet CAD package [17], which is based on the variational energy minimization technique to solve the magnetic vector potential. The partial differential equation for the magnetic vector potential is given by [18],

$$-\frac{\partial}{\partial x}\left(\gamma\frac{\partial A}{\partial x}\right)-\frac{\partial}{\partial y}\left(\gamma\frac{\partial A}{\partial y}\right)=J \qquad (1)$$

where, A is the magnetic vector potential.

In the variational method (Ritz) the solution to 1 is obtained by minimizing the following

$$F(A)=\frac{1}{2}\iint_{\Omega}[\gamma(\frac{\partial A}{\partial x})^2+\gamma(\frac{\partial A}{\partial y})^2]d\Omega-\iint_{\Omega}JAd\Omega \qquad (2)$$

where $\Omega$ is the problem region of integration.

In the finite element analysis second order triangular elements with dense meshes at places where the variation of fields are greater have been used.

The plots of magnetic field density and magnetic flux for only field coil considered to be turned on and having 0.25 A are shown in Figure 6.

In order to be able to analyze the motor in two dimensions, the normal field boundary conditions are used over the inner and outer borders of the motor. Figures 7 and 8 show the magnetic flux and the magnetic field density for aligned and non-aligned cases for a field current of 0.25 A and the stator winding current of 3 A.

The plot of static torque versus rotor positions developed by the hybrid brushless dc motor is shown in Figure 9.

The Torque versus angle characteristics of the motor are obtained by using the finite element method in which giving a constant current in two phases of the motor occur in an appropriate switching cycle.

There is a discussion on the static torque vs. position for BLDC motor in [19] which models the effects of skewing in BLDC motor on its performance. It is worth mentioning here that, the stator and rotor cores are made of a non-oriented silicon steel lamination. The magnetization curve is taken from the manufacturer's data sheet for M-27 steel. In Figure 9 zero degrees is considered as an unaligned case.

Due to the motor being new in its class, a new drive circuit having independent bidirectional control for each motor phase arises.

## 4. THE NEW DRIVE CIRCUIT

Due to the motor being new in its class, this drive circuit utilizes four power switches in the form of a bridge connection for each motor phase. This type of connection provides the bidirectional current flow for each phase at any time independently. Therefore, the motor can operate by switching to different sequences for the current direction in each motor phase windings and also offers the choice of having any number of phases to be turned on at any time. This technique provides different control schemes for testing a motor with only one converter topology. There are three methods to run the motor, depending on how many phases to be turned on at a time in the proper direction. The method used in this paper

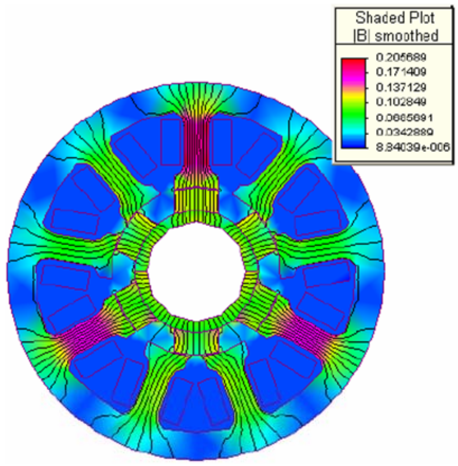


**Figure 6**. Plots of magnetic field density and magnetic flux.

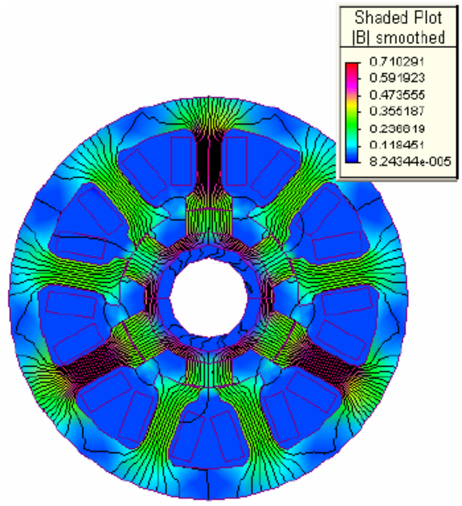


**Figure 7**. Plots of magnetic field density and magnetic flux for aligned case.

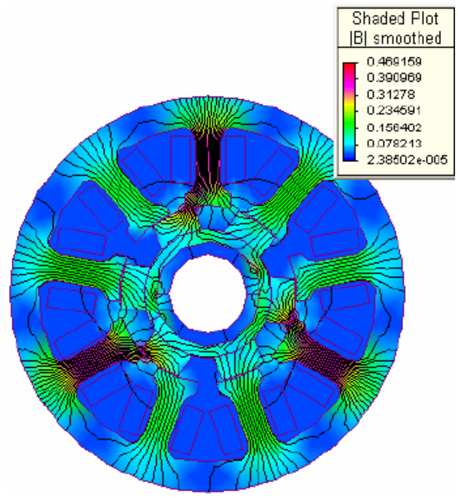


**Figure 8**. Plots of magnetic field density and magnetic flux for non-aligned case.

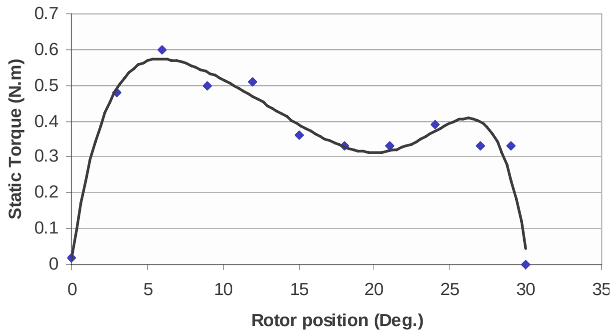


**Figure 9**. Static torque versus rotor angle.

uses two phase turn ons at a time namely, one in attracting and the other one in repelling modes, respectively. A sketch of the drive circuit is shown in Figure 10.

There are three methods to run the motor, depending on how many phases to be turned on at a time in the proper direction. The method used in this paper utilizes two phase turn ons at a time namely, one in attracting and the other one in a repelling mode, respectively.

Figure 11a shows the voltage on one of the motor phases while Figure 11b shows the current using the new drive circuit.

As shown, the voltage is positive, zero and negative for one third of the period and the current reverses direction during that time.

Figure 12 shows the actual phase commands produced by the drive circuit to two of the H-bridge power transistors.

The overlapping between the two successive phases is clearly shown in Figure 12.

Finally, Figure 13 shows the input current into the motor from the supply voltage.

The current increases when the phase is on and then decreases as the phase is turned off.

In BLDC motors, each individual phase excitation must be synchronized with the rotor position which necessitates the need for a position sensing scheme. In general there are two types of rotor position sensing methods namely, direct and indirect. In the direct position the sensing method , usually a mechanical shaft position transducer, such as Opto-couplers with a slotted disk, Hall-

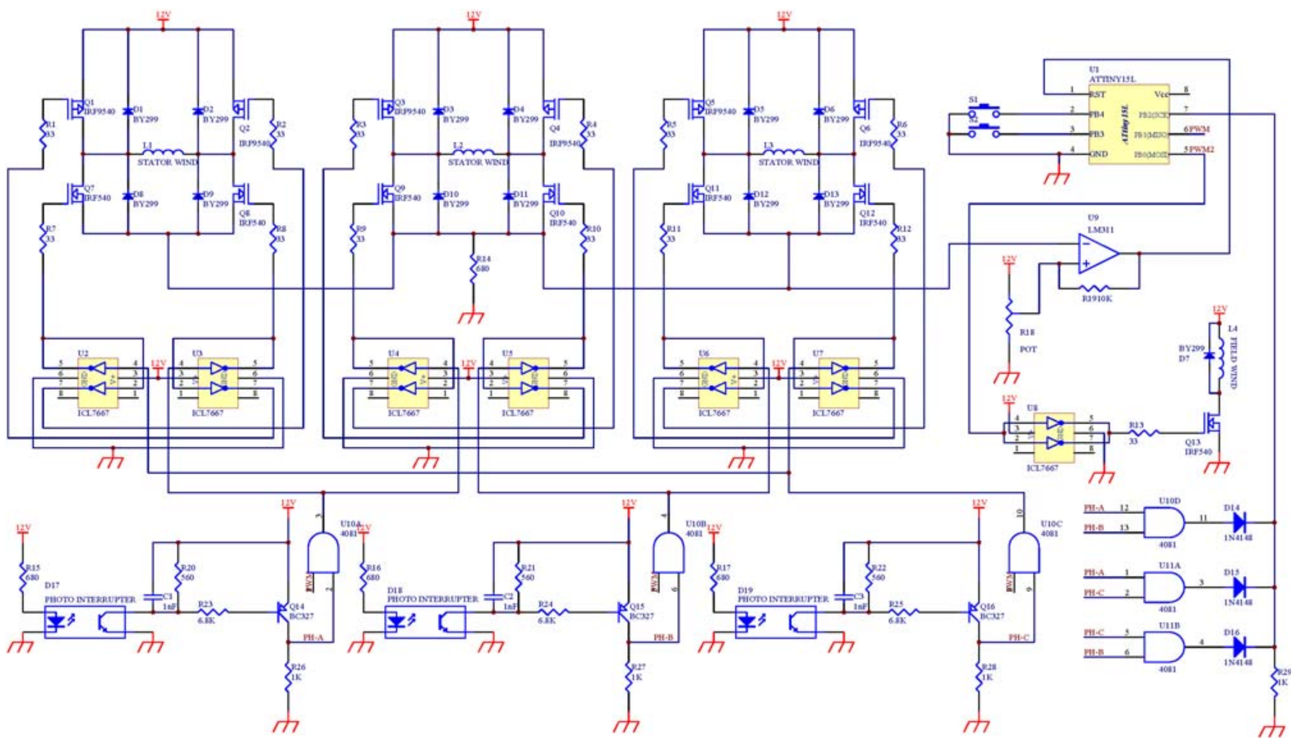

**Figure 10**. The drive circuit.

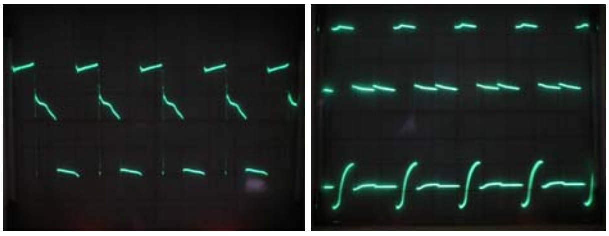

(a) (b)

**Figure 11**. (a) The phase voltage 10v/div, 0.2 ms/div and (b) The phase current 1v/div, 0.2 ms/div.

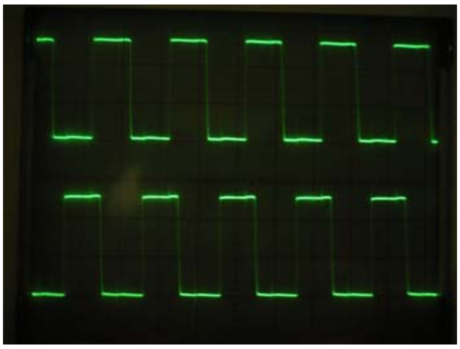

**Figure 12**. The actual phase commands produced by the drive circuit for two successive phase. 2v/div, 0.2 ms/div.

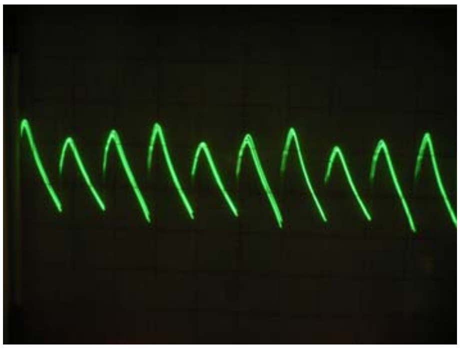

**Figure 13**. The input current into the motor 1v/div, 0.2 ms/div.

effect sensors and embedding permanent magnets within the teeth of the slotted disk, or a high precision encoder is mounted on the motor housing to produce the necessary and accurate rotor position information for the proper motor operation. Figure 14 shows Opto-couplers with a slotted disk together used in detecting the rotor position for the new brushless dc motor.

The output signals come from the photo-interrupters mounted on the back of the motor. There are three $30^o$ pulses produced by the motor shaft position sensors and each pulse appears 6 times in one rotation. Figure 15a shows the resulting pulses produced by the sensing unit for $30^o$ duration while 15b shows two consecutive photo-interrupters.

In Figure 15a there is no overlapping between the phases and each photo-interrupter works one third of the period. In Figure 15b the overlapping of the two photo-interrupters output signals which corresponds to two of the motor phases to be on at one time is clearly shown. It is possible to adjust the unit for any overlapping needed.

## 5. EXPERIMENTAL RESULTS

The motor has been fabricated and tested for performance and functionality in the laboratory. Figure 16 illustrates the novel brushless dc motor fabricated in the laboratory.

The static torque of the motor was obtained by blocking the motor at a different angle. The average static torque for a rated current of 3 A was measured to be about 46 N.cm over the stator pole arc (0 to $30^0$). It suddenly went to zero at the start of stator to rotor complete overlap. It was observed that the static torque shows lower value than computed which is expected, since, the silicon sheet steel material used to build the motor is not quite what is used for the numerical analysis.

Using a motor generator assembly, the dynamic torque for the motor versus the speed has been measured by loading the motor. The torque speed characteristics of the motor for two different field currents is shown in Figure 17.

The power curve fitting has been used for the data points. The torque speed characteristics of the motor behave like a series of dc motors and switched reluctance motor.

Figure 18 shows the plot of the motor torque versus the current under different loads for the motor.

As seen from the Figure 16 the torque is

**Figure 14**. Plots of magnetic field density and magnetic flux.

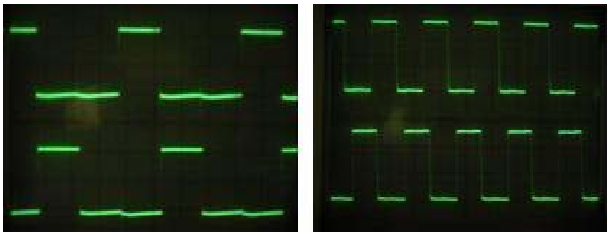

(a) (b)

**Figure 15**. (a) The output signals from the photo-interrupters and (b) Resulting pulses from two consecutive photo-interrupters.

**Figure 16**. The actual brushless dc motor.

proportional to the square of the motor current which resembles the switched reluctance motor.

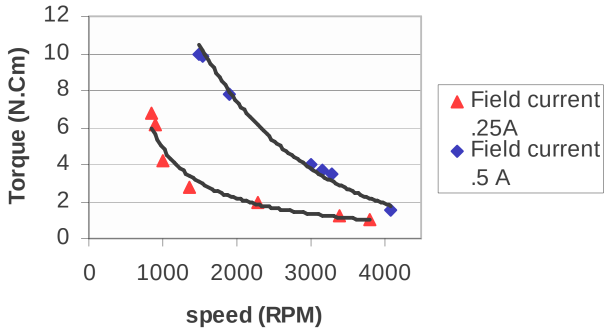


**Figure 17**. Dynamic torque of the motor versus speed.

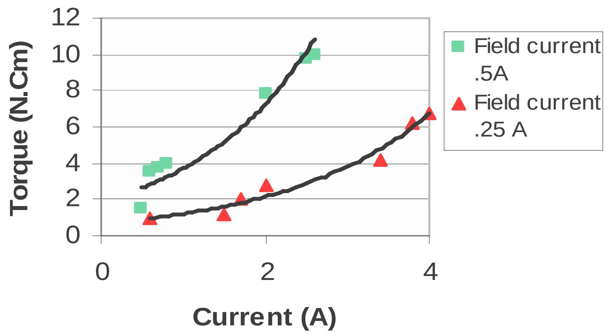


**Figure 18**. Plot of the motor torque versus current.

The static torque versus the rotor position is also obtained by using a torque meter which generally agrees with the one found numerically.

The shaft of the motor/generator machine is connected to a motor to act as a prime mover. The speed of the motor is kept constant first, at 1000 and then at 2000 rpm under different loads for various field currents. The results of these tests are shown in Figures 19a and 19b.

In these figures curve fitting (power) has been used for better presentation of the data points. The actual output voltages for two consecutive phases are also shown in Figure 20.

Figures 21a and 21b show the output voltages from one phase of the generator for a field current of 0.25A and 0.5A, respectively.

The voltages have harmony which is due to the shape of the stator and rotor poles. Finally, Figure 22 shows the actual motor/generator unit plus the drive circuit.

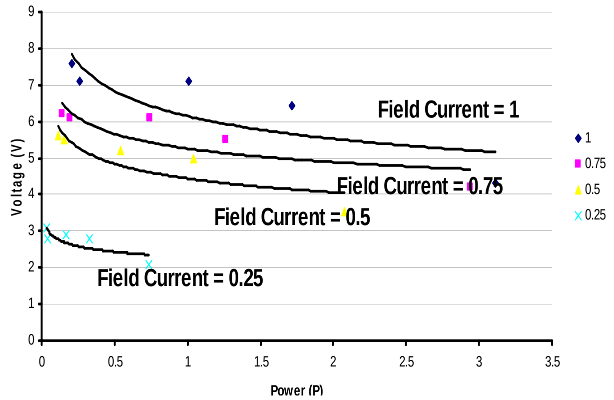


(a)

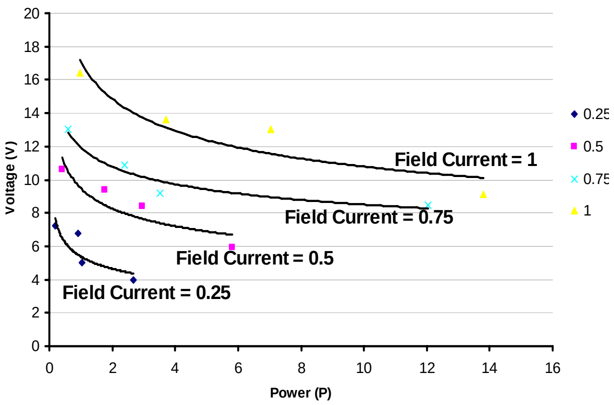


(b)

**Figure 19**. (a) Output voltage vs. power (1000 rpm) and (b) Output voltage vs. power (2000 rpm).

(a) (b)

**Figure 21**. Output voltage from one phase of the generator (a) Field current of 0.25 A and (b) Field current of 0.5 A.

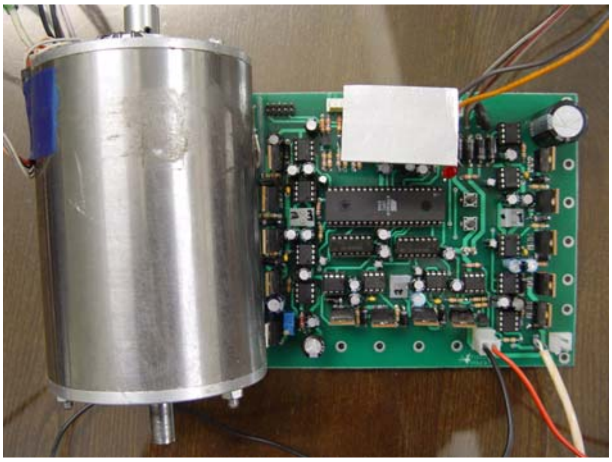

**Figure 22**. The actual motor/generator unit and the drive circuit.

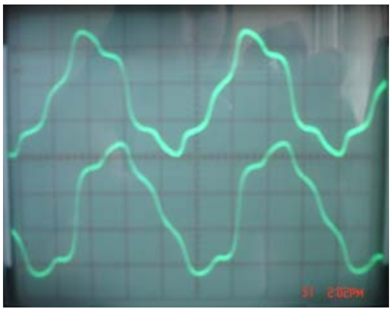

**Figure 20**. Plots of magnetic field density and magnetic flux.

## 6. CONCLUSION

In this paper a novel brushless dc motor/generator plus a drive circuit were designed and fabricated in the laboratory. The motor was numerically analyzed and some of its parameters experimentally measured and tested. The two main objectives of this paper namely, introduction of a new motor/generator configuration without a permanent magnet and also introducing a drive circuit having independent bidirectional control for each phase were achieved. The result of finite element analysis is in close agreement (within 20 percent) with the experimental outcome. The discrepancy is due to utilizing different (but close) a magnetization curve in the numerical analysis and also using a two dimensional analysis instead of a three dimensional one. The highest efficiency obtained for the unit was around 42 %.

This motor/generator could potentially be used in electric vehicles because it does not use a permanent magnet in its construction therefore it is very durable. The generator output voltage can be simply kept constant under different speeds contrary to PM brushless dc motors since; the field current is easily controllable.

## 7. REFERENCES


1 Kusko, A. and Peeran, S. M., "Definition of the Brushless DC Motor", ***IEEE Transaction on Industry Appl***., (1988), 20-22.

2 Hanselman, D. C., "Brushless Permanent Magnet Motor Design", McGraw-Hill, New York, 1994.

3 Matsuoka, K. and Obata, S., "Automatic Design Method of Brushless DC Motors for VCRS", ***IEEE Transactions on Consumer Electronics***, Vol. 35, No. 3, (August, 1989), 642-648.

4 Miller., T. J. E., "Brushless Permanent-Magnet and Re1uctance Motor Drives", ***Science Publications***, Oxford, England, (1989).

5 Hang, D. R., Fan, C. Y., Wang, S. J., Pan, H. P., Ying, T. F., Chao, C. M. and Lean, E. G., "A New Type of Single-Phase Spindle Motor for HDD and DVD", ***IEEE Transactions on Magnetics***, Vol. 35, No. 2, (March, 1999), 839-845.

6 Mayer, J. S. and Wasyezuk, O., "Analysis and Modeling of Single-phase Brushless DC Motor Drive System", ***IEEE Transaction on Energy Conversion***, Vol. 4, No. 3, (September, 1989), 473-478.

7 Rahman, K. M., Fahimi, B., Suresh, G., Rajarathnam, A. V. and Ehsani, M., "Advantages of Switched Reluctance Motor Applications to EV and HEV: Design and Control Issues", ***IEEE Trans. Industry Applications***, Vol. 36, (2000), 111-121.

8 Emadi, "Low-Voltage Switched Reluctance Machine Based Traction Systems for Lightly Hybridized Vehicles", ***Society of Automotive Engineers***, (2001), 1-7.

9 Lehmann, K. J., Probst, G. and Schäfer, H., "The Integrated Starter Generator as Part of the Power Train Management", ***Aachener Kollequium Fahrzeug-und Motorentechnik***, (2000), 11-11.

10 Fahimi, B. and Emadi Jr., A. R. B., "A Switched Reluctance Machine Based Starter/Alternator for More Electric Cars", ***IEEE Transactions on Energy Conversion***, Vol. 19, (March, 2004), 116-124.

11. Boldea, I., Tutelea, L. and Pitic, C., "PM-Assisted Reluctance Synchronous Motor/Generator (PM-RSM) for Mild Hybrid Vehicles: Electromagnetic Design", ***IEEE Transactions on Industry Applications***, Vol. 40, No. 2, (March, 2004), 492-498.

12. Gopalarathnam, T. and Toliyat, H. A., "A New Topology for Unipolar Brushless DC Motor Drive with High Power Factor", ***IEEE Transactions on Power Electronics***, Vol. 18, No. 6, (November, 2003), 1397-1404.

13. Bass, J. T., Ehsani, M. and Miller, T. J., "Development of a Unipolar Converter for Variable Reluctance Motor Drives", ***IEEE Transactions on Industry Applications***, Vol. IA-23, (1987), 545-553.

14. Krishnan, R. and Vijasraghavan, P., "A New Power Converter Topology for PM Brushless DC Motor Drives", ***Con. Record, IEEE-IEE Con.***, (1998), 709-714.

15. Krishnan, R., "A Novel Single-Switch-per-Phase Converter Topology for Four Quadrants PM Brushless DC Motor Drive", ***IEEE Trans. on Industry Applications***, Vol. 33, No. 5, (1997), 1154-1161.

16. Upadhyay, R. and Rajagopal, K. R., "FE Analysis and CAD of Radial-Flux Surface Mounted Permanent Magnet Brushless DC Motors", ***IEEE Transactions on Magnetics***, Vol. 41, No. 10, (October, 2005), 3952-3954.

17. Magnet CAD Package: User Manual, Infolytica Corporation Ltd., Montreal, Canada, (2001).

18. Demerdash, N. A. O. and Alhamadi, M. A., "Three Dimensional Finite Element Analysis of Permanent Magnet Brushless DC Motor Drives-Status of the State of the Art", ***IEEE Transactions on Industrial Electronics***, Vol. 43, No. 2, (April, 1996), 268-276.

19. Alhamadi, M. A. and Demerdash, N. A., "Modeling of Effects of Skewing of Rotor Mounted Permanent Magnets on the Performance of Brushless DC Motors", ***IEEE Transactions on Energy Conversion***, Vol. 6, No. 4, (December, 1991), 721-730.